Evaluation of SUVlean Consistency in FDG and PSMA PET/MR with Dixon, James and Janma Based Lean Body Mass Correction

Jun Zhao (petcenter@126.com)
Shanghai East Hospital https://orcid.org/0000-0002-9887-5512
Qiaoyi Xue
Central Research Institute, United Imaging Healthcare Group, Shanghai
Xing Chen
Department of Nuclear Medicine, Shanghai East Hospital, Shanghai
Zhiwen You
Shanghai First People's Hospital Department of Nuclear Medicine
Zhe Wang
Central Research Institute, United Imaging Healthcare Group, Shanghai
Jianmin Yuan
Central Research Institute, United Imaging Healthcare Group, Shanghai
Hui Liu
Central Research Institute, United Imaging Healthcare Group, Shanghai
Lingzhi Hu
Central Research Institute, United Imaging Healthcare Group, Shanghai

Original research

Keywords: SUV, Consistency, FDG, PSMA, PET/MR

Posted Date: November 10th, 2020

DOI: https://doi.org/10.21203/rs.3.rs-103354/v1

Version of Record: A version of this preprint was published on February 17th, 2021. See the published version at https://doi.org/10.1186/s40658-021-00363-w.

Evaluation of SUVlean consistency in FDG and PSMA PET/MR with Dixon, James and Janma based lean body mass correction

Jun Zhao1#, *, Qiaoyi Xue2#, Xing Chen1, Zhiwen You1,Zhe Wang2, Jianmin Yuan2, Hui Liu2, Lingzhi Hu2

1. Department of Nuclear Medicine, Shanghai East Hospital, Tongji University School of Medicine, Shanghai, China

2. Central Research Institute, United Imaging Healthcare Group, Shanghai, China

* Author for correspondence

# Jun Zhao and Qiaoyi Xue contributed equally to this work.

Jun Zhao, Email: petcenter@126.com

Abstract

Purpose To systematically evaluate the consistency of various standardized uptake value (SUV) lean body mass (LBM) normalization methods in a clinical positron emission tomography/magnetic resonance imaging (PET/MR) setting.

Methods SUV of brain, liver, prostate, parotid, blood and muscle were measured in 90 ^{18}F-FDG and 28 ^{18}F-PSMA PET/MR scans and corrected for LBM using the James, Janma (short for Janmahasatian) and Dixon models. 40 dual energy X-ray absorptiometry (DXA) measurements of non-fat mass were used as the reference standard. Agreement between different methods was assessed by linear regression and Bland-Altman statistics.

Results LBM fraction measured by DXA, James, Janma and Dixon approaches was 68.19±6.43%, 66.95±6.71%, 76.20±5.41% and 71.56±7.97% respectively. Compared to DXA, the Dixon approach presented the minimal bias when compared to the James and Janma models (bias: 0.76±7.35, -8.01±9.36, -3.33±8.26 respectively). SUV normalized by bodyweight (SUVbw) was positively correlated with Body Mass Index (BMI) in both FDG (liver: $r=0.454$, $p<0.001$) and PSMA studies ($r=0.197$,$p=0.31$), while SUV normalized by lean body mass (SUVlean) revealed a decreased dependency on BMI ($r=0.22,0.08,0.14$, $p=0.04,0.46,0.18$ for Dixon, James and Janma models respectively). Paired T-test showed significant difference between SUVlean of major organs measured using Dixon method vs James and Janma models.

Conclusion Significant systematic variation was found among SUVlean calculated using different approaches. A consistent correction method should be applied in PET/MR serial scans.

Keywords: SUV, Consistency，FDG, PSMA, PET/MR

Declarations

Funding Information

Key Specialty Construction Project of Pudong Health and Family Planning Commission of Shanghai, PWZzk2017-24. Project of Science and Technology Commission of Shanghai Municipality, 19DZ1930703.

Conflict of interest

Qiaoyi Xue, Zhe Wang, Jianmin Yuan, Hui Liu, Lingzhi Hu are the employees of United Imaging Healthcare. The other authors declare that they have no conflict of interest.

Ethical approval

All procedures performed in studies involving human participants were in accordance with the ethical standards of the institutional and/or national research committee and with the principles of the 1964 Declaration of Helsinki and its later amendments or comparable ethical standards.

Consent to participate

Informed consents were obtained from the patients for the anonymous use of ther clinical, imaging, and histologic data for publication.

Consent for publication

Written informed consent for publication was obtained from all participants.

Availability of data and material

Not applicable.

Code availability

Not applicable.

Acknowledgements

We would like to thank the financial support from key research program (2016YFC0103900), Ministry of Science and Technology of People's Republic of China and Key Specialty Construction Project of Pudong Health and Family Planning Commission of Shanghai. We also thank Dr. Adam Chandler from United Imaging America for proof-reading.

Introduction

With the development of integrated positron emission tomography/magnetic resonance imaging (PET/MR), its comprehensive contrast mechanisms and seamless fusion of morphology and function is attracting growing clinical adoption and research exploration. Because of the reduced radiation dose of PET/MR versus PET/CT, and the increasing utilization of non-FDG (fluorodeoxyglucose) tracers, such as PSMA (Prostate Specific Membrane Antigen) and DOTATATE [1, 2], serial PET/MR scans are becoming more desired for re-staging and treatment response evaluation for oncological patients. Serial PET scans require higher standards for the quantitation consistency as patients might present dramatic physiological variation in terms of body weight throughout the course of treatment [3].

In PET studies, standardized uptake value (SUV) is the most widely used semiquantitative measurement of radiotracer uptake, which is essential for diagnosis and treatment response assessment. SUV is defined as the radioactivity in a region of interest (ROI) normalized by the total injected dose and body weight of the patient [4]. Although SUV normalized by body weight (SUVbw) is the most popular metric in today's clinical setting, Zasadny et al found that it is highly dependent on patient weight and body fat content [5]. A potential cause of inconsistency is that white adipose tissue contributes to body weight but poses minimal uptake of radiotracer. SUVbw is occasionally overestimated (especially for obese subjects) and can lead to systematic bias for serial scans of patients with multiple follow-ups throughout the course of treatment [6]. Many studies have investigated improved normalization factors of SUV to allow for consistent quantitation across a wide range of body mass index (BMI) [7, 8]. The most widely adopted approach is to use lean body mass (LBM) instead of body weight to offset the systematic bias caused by white adipose tissue [5]. This corrected SUV is often referred as SUVlean.

Over the past decades, various predictive models have been established to estimate LBM, taking factors such as body weight, height, sex or age into account. Some of these models have been translated into PET imaging to calculate SUVlean in the clinical setting [5, 7-9]. Among them, James equation [10] is the most widely used model for SUV correction and has been implemented into a large variety of commercially available PET/CT and PET/MR scanners. However, a recent study has shown that James equation might be prone to significant inaccuracy when a patient's BMI exceeds a critical value (approximately 43 for men and 37 for women) [11]. An improved model proposed by Janmahasatian et al [12] was adopted by a recent study [11] to improve the SUV consistency for patients with high BMI. However, even though model-based lean body mass estimation was derived from extensive clinical data containing a large patient cohort, there are still concerns that the predictive formula may cause substantial errors at the individual level. For instance, two patients with the same weight and height exhibit identical LBM values but may present significantly different body fat composition.

New LBM estimate approaches based on direct measurement using CT or MR in PET/CT and PET/MR [13-15] are believed to be more reliable than model-based LBM calculation [16]. In multi-modal PET/MR imaging, current state of the art MR based attenuation correction (MRAC) usually employs water/fat imaging using a Dixon sequence [17] and such data can be readily utilized to achieve personalized calculation of LBM. The Dixon approach was recently proposed and validated in a pilot study, where

Jochimsen et al reported an initial attempt to normalize SUV with the Dixon based water/fat fraction [18].

Furthermore, without cross-validation with clinical reference standards for LBM, it remains challenging to conduct direct evaluation of the accuracy of SUVlean [19]. One approach for validating and comparing different SUV normalization models is to utilize reference standard measurements of LBM using well-established technology [16, 20]. There are many ways to measure body fat and its distribution [21]. For instance, dual energy X-ray absorptiometry (DXA) utilizes different attenuation coefficient of fat and soft tissue to obtain a patient-specific fat fraction [22]. DXA has been reported to be more accurate than density-based methods and features good repeatability in which regional fat fraction can be obtained by cropping the projected 2D coronal image [23].

Although a few recent studies have reported good reproducibility of Dixon methods [24] and good agreement between Dixon and DXA measurements of body fat [15, 25, 26], the robustness of the PET SUV corrected by Dixon methods has not been well evaluated. In addition, because of the diverse selection of methods to calculate lean body mass for SUVlean, there is an immediate need for comparative evaluation of the consistency and limitation across these methods for SUVlean calculation in PET/MR. The purpose of the present work is to systematically evaluate the accuracy of different LBM estimation models, using DXA as a reference standard, and to investigate the consistency of various SUVlean calculation methods in a clinical setting. SUVlean measurements derived from Dixon images, as well as with James and Janma (short for Janmahasatian) LBM models were compared in two patient cohorts of ^{18}F-FDG and ^{18}F-PSMA PET/MR studies, respectively.

Materials and methods

Patient Population

Patients (N=118) were recruited for clinical PET/MR scans from December 2018 to August 2020 at Shanghai East Hospital for suspected or known malignancies. Among them, 90 underwent ^{18}F-FDG PET/MR scans and 28 underwent ^{18}F-PSMA PET/MR scans. 40 out of 118 patients were enrolled in a same day DXA scan for body fat measurement. Patient weight ranged from 37 to 103 kg and BMI ranged from 14.53 to 32.45. Detailed information of the patients is provided in Table 1. The study protocol was reviewed and approved by institutional review board (IRB) and written informed consent was obtained from each patient.

PET/MR Image Acquisition

Whole-body PET/MR scans were performed on a hybrid PET/MR (uPMR 790, UIH, Shanghai, China), which consisted of a 3.0T MR and PET system with a transverse field of view of 60cm and axial field of view of 32cm. The PET system comprises 112 rings, each containing 700 15.5×2.76×2.76 mm^3 LYSO crystals [27]. All patients were requested to fast for at least 6 hours before the injection of the radioactive tracer. For the FDG study, patients were injected with 221±50MBq (or 0.096±0.017mCi/kg) of ^{18}F-FDG and rested in a quiet preparation room for about 1 hour. For the PSMA study, patients were injected with 314±73MBq of ^{18}F-PSMA-1007 and rested for about 2 hours.

Images were acquired using the clinical PET/MR protocol at Shanghai East Hospital.

During the PET scan, a 2-point Dixon based water-fat separation imaging sequence was performed simultaneously using a 3D T1-weighted gradient echo sequence with compressed sensing (TE=2.24ms, TR=4.91ms, flip angle=10, echo train length=30, FOV=549×384, matrix=256×329, slice thickness=2mm, slice spacing=2mm, transverse plane). The PET/MR attenuation correction (MRAC) map was generated by segmenting the Dixon images into water, fat, lung and air and assigning attenuation coefficients of 0.096, 0.08, 0.032, and 0 cm^{-1}, respectively. Representative images of FDG and PSMA PET/MR are shown in Fig. 1 & 2.

DXA Image Acquisition

DXA images were obtained using a dual-energy X-ray absorptiometry (DXA) (Lunar Prodigy, GE, Madison, USA) and body composition was analyzed using the vendor-provided software (enCORE, GE, Madison, USA). Since the PET/MR scans only covered from skull to the upper thigh, the ROI of the DXA images were adjusted to obtain the total mass and fat mass for the same axial coverage as the PET/MR images.

LBM Calculation

The total volume of water, fat, lung and air were obtained from the Dixon MRAC images by multiplying the total number of voxels by the voxel volume for each compartment. We first compared volumes of fat and water with the mass derived from DXA analysis to assess the agreement between the two measurements by linear regression. A population-based water and fat density were derived by linear fitting the volume versus measured water and fat mass from DXA.

Model-based LBM were calculated using James equation and Janma equation respectively,
where

$$LBWjanma = \begin{cases} {9270 * BW}/{6680 + 216 * BMI} \ , \ Men \\ {9270 * BW}/{8780 + 244 * BMI} \ , Women \end{cases} \quad (1)$$

and,

$$LBWjames = \begin{cases} 1.1 * BW - 128 * (\frac{BW}{height})^2, Men \\ 1.07 * BW - 148 * (\frac{BW}{height})^2, Women \end{cases} \quad (2)$$

and compared with the direct measurement result from DXA as the reference standard.

PET Reconstruction and SUV Measurements

All PET reconstructions and image analysis were performed on the vendor-provided workstation (uPMR 790, UIH, Shanghai, China). The PET images were reconstructed using the ordered subset expectation maximization (OSEM) algorithm (FOV=600mm, iteration=2, subsets=20, Gaussian filter with FWHM=4mm, matrix size=150). Soft tissue radioactivity of major organs was measured by drawing ROIs on the workstation. Specifically, the radioactivity of the liver was obtained by placing a 3 cm diameter spherical volumetric ROI in the right hepatic lobe avoiding major vessels/lesions. The radioactivity of the blood pool was obtained by placing a 0.1 cm diameter spherical ROI in the left ventricle of the heart and the muscle SUV was obtained from the right thigh. Brain radioactivity in the FDG studies was obtained by thresholding out the whole brain using an in-house algorithm which was

then subsequently validated by visual inspection. Prostate and parotid glands in the PSMA studies were detected by a thresholding tool available in the workstation software.

SUVbw was calculated by the default settings in the workstation as:

$$SUVbw = \frac{radioactivity\ in\ ROI(kBq/ml)}{injected\ dose(MBq)*decay\ factor/bodyweight(kg)} \quad (3)$$

,where decay factor=exp(-0.693*wait time/radionuclide half-life).

SUVlean calculated using Dixon, James and Janma approaches were denoted as SUV_dixon, SUV_james and SUV_janma, respectively.

SUV_dixon was calculated as:

$$\text{SUV\_dixon} = SUVbw * \frac{water\ mass}{water\ mass+fat\ mass+lung\ mass} \quad (4)$$

,where water and fat mass were derived from the Dixon MRAC images.

SUV_james was calculated as:

$$\text{SUV\_james} = SUVbw * LBWjames/bodyweight \quad (5).$$

Finally, SUV_janma was calculated as:

$$\text{SUV\_janma} = SUVbw * LBWjanma/bodyweight \quad (6).$$

Statistical Analysis

Linear regression and Bland-Altman analysis were used to evaluate the accuracy of different LBM measurements. LBM calculated from Dixon, James and Janma approaches were compared with the DXA results as the reference standard. Scatter plots with linear regression were performed to interpret the relationship between the different types of SUVlean and BMIs. Linear regression with a F-test was used to assess the dependency of SUVbw and different forms of SUVlean on BMI. All statistical analysis was performed in Matlab 2018b (MathWorks, Natick, Massachusetts, USA), Excel 2016 (Microsoft, Seattle, USA) and GraphPad Prism 8.0.2 (GraphPad Software, California, USA).

Results

DXA vs Dixon

The average body weight for 20 female subjects was 58.6±8.7 kg and the average body weight for 20 male subjects was 69.2±12.8 kg. The average BMI for women was 22.6±3.2 and average BMI for men was 24.3±4.3. The mean non-fat mass of the head-to-thigh region obtained in DXA was 30.14±3.9 kg for women and 43.47±7.86 kg for men. The corresponding total water volume obtained by Dixon was 247.2±3.1L for women and 337.7±6.4L for men.

The slope from the linear regression was 0.78 and 1. 26 for fat and water, with r^2=0.849 and 0.915 respectively, suggesting excellent agreement between the measurements of DXA and Dixon (Fig. 3a).

To convert MRI measured volumes to weight in the recruited patient population, lung volumes were taken into account for multi-parameter linear regression, yielding coefficients (densities) of 0.79, 1.23 and 0.20 for fat, water and lung respectively. Using the derived tissue density, the fat and water mass was determined as 17.38±5.05 kg and 33.50±6.84 kg from Dixon images. The Bland-Altman plot of fat fraction and water mass fraction are shown in Fig. 3b.

LBM Fraction

The measured LBM fraction using DXA were 63.01±3.91%, 73.37±3.71% and 68.19±6.43% for females, males and all patients. As summarized in Table 2, LBM fraction calculated using Dixon images, James model and Janma model were measured to be 62.68±5.74%, 73.59±4.82% and 65.08±3.67% for female patients, 71.22±4.59%, 78.80±4.74%, and 77.95±5.45% for male patients, 66.95±6.71%, 76.199±5.406% and 71.56±7.97% for all patients. Excellent linear correlation was found between calculated LBM fraction and DXA reference standard using all methods, while the Dixon approach presented minimal bias compared to the James and Janma models.

SUV in FDG study

Linear regression between FDG SUVbw and SUVlean calculated using different approaches of LBM was plotted in Fig. 4 and the quantitative statistical results were summarized in Table 3. SUVbw was found to be significantly ($p<0.05$) positively correlated with BMI for all organs except for the SUVbw max value in the brain. The dependency on BMI was eliminated using Dixon, James and Janma-based SUVlean calculations as demonstrated by the reduced slope and F-test values. Paired T-test showed significant difference between SUVlean measured using Dixon approach vs James and Janma models.

SUV in PSMA study

SUVbw was found significantly ($p<0.05$) positively correlated with BMI for mean value within the blood pool and muscle while not statically significant within other organs measured. The dependency on BMI was eliminated using Dixon, James and Janma-based SUVlean calculations as demonstrated by the reduced slope. Paired T-test showed significant difference between SUVlean measured using Dixon methods vs James and Janma models. Linear regression between PSMA SUVbw and SUVlean is shown in Fig. 5 and quantitative statistics results are summarized in Table 4.

Discussion

Quantitation of tracer uptake in PET/MR image is essential for cancer staging and treatment response evaluation in both clinical and research settings. The pitfall of the widely used SUVbw is that it is highly dependent on patient weight and may overestimate the uptake of obese patients [5]. It has been reported that SUVbw was 70% higher in high-weight patients than in low-weight patients, and the overestimation was reduced when using other SUV normalization factors [6]. Using LBM instead of full body weight can effectively eliminate this effect and improve consistency among patients. Our findings in the FDG study were consistent to those reported by Zasadny [5] and Wahl [7, 11]. Our findings in the PSMA study were also in line with previously reported results [28]. However, it is notable that, even though multiple approaches all achieved satisfactory correction for the BMI dependency of SUV, significant differences were found among Dixon, James and Janma approaches.

Using DXA as the reference standard, this study compared for the first time the accuracy of the three widely used approaches to estimate LBM. All three methods were found in good agreement with DXA, but Dixon offered the highest accuracy due to its direct measurement of body composition. James and Janma models might be prone to individual bias due to the fact that BMI might not be fully indicative of body fat content, even though they both offer reasonable population-based estimates of body fat content in the recruited cohorts from our study.

The Dixon approach offers quantitative measurement of body water/fat volume from MRI images and has gradually established itself as an alternative LBM standard [24]. Jochimsen et al [18] first proposed a method to correct SUV using water-fat signal fraction of Dixon scans in 2015. In the present work, we revised their method to be more straight-forward and easy-to-implement and validated it using a larger patient cohort and an additional tracer. Our method is different from Jochimsen's in that we utilized DXA measurements to transfer volume units into mass units, whereas they used signal intensity fraction instead.

It is notable that in previous reports [11], both body weight and BMI can be utilized as the dependent variable for SUV when evaluating the impact of obesity on SUV accuracy. We used BMI as the factor reflecting patient adiposity in our study because it is more indicative of actual fat content than body weight. For instance, patients from our cohort exhibited a wide range of body size but the most obese subject with the highest BMI was of moderate bodyweight (80kg) but very short in height (1.52m). Therefore, weight may not be an ideal parameter to indicate the degree of obesity and we used BMI ($BMI=weight/height^2$) as an indicator of obesity instead.

It is worthwhile mentioning that even though all three LBM approaches can be utilized to correct for the BMI dependency of SUV in FDG and PSMA studies, significant variation still exists among different approaches. A potential cause is that all empirical models including James and Janma are derived from specific patient populations while Dixon is a direct measurement of body composition. In serial PET/MR scans where quantitative accuracy is crucial, a consistent SUVlean calculation approach should be adopted to correct for the change of body weight and BMI index to minimize systematic bias.

There are a few limitations in this study. Firstly, since we were using 2-point Dixon which is the basic form of Water Fat Imaging (WFI), we could only obtain the total amount of body fat by summing the total number of categorized voxels. Further work might involve the use of more advanced WFI sequences (e.g. 6-point Dixon) that can differentiate different types of adipose tissue and derive the fat content within a single voxel. Brown adipose tissue that is typically active in glucose metabolism [29, 30] should not be subtracted from LBM. Secondly, although SUV dependency on BMI in the PSMA study was also positive, correlation between SUV and BMI in most organs (except for blood pool) were not statistically significant. This could be due to the limited number of patients enrolled in this study. In a recent work by Grafita et al [28], a weak but significantly positive correlation was observed between liver SUV and body weight among 121 patients who underwent 68Ga-PSMA PET/CT. The SUVlean normalized by Janma LBM was reported to have a reduced correlation with body weight. Finally, we did not include lesion uptake in this work because it is heterogenous in nature and subject to the impact of biochemistry of specific patients. The uptake of lesions depends mostly on characteristics of the tumor itself, such as tumor stage, size, degree of aggressiveness and histology type.

Conclusion

In this study we have compared LBM calculated using Dixon, James, and Janma approaches and validated their accuracy using DXA measurement. All three methods offer good estimates of LBM ratio with Dixon offering the best agreement with DXA. SUVbw was found to be positively correlated with BMI in the FDG and PSMA patient populations while SUVlean calculated using Dixon, James and Janma confirmed a decreased dependence on BMI. However, significant systematic variation was found among SUVlean calculated using different approaches, suggesting that a consistent correction method would be needed in PET/MR serial scans.

Figs & tables

Fig. 1 Representative images from a ^{18}F-FDG PET/MR scan. **a** PET MIP, **b** water image, **c** fat image, **d** in-phase image, **e** MRAC map, **f** water segmented from MRAC, **g** fat segmented from MRAC and **h** lung segmented from MRAC.

Fig. 2 Representative images from a ^{18}F-PSMA PET/MR scan. **a** PET MIP, **b** water image, **c** fat image, **d** in-phase image, **e** MRAC map, **f** water segmented from MRAC, **g** fat segmented from MRAC and **h** lung segmented from MRAC.

Fig. 3 a: Linear regression of volume measured by Dixon vs. mass measured by DXA covering from head to upper thigh. The solid line interprets the linear fit of the data and dotted line represents 95% confidence interval of the model. **b**: Bland-Altman plot showing agreement between fat mass/bodyweight of DXA and Dixon measurements, and water mass/bodyweight of DXA and Dixon measurements.

Fig. 4 Linear regression of different types of SUV measurements as a function of BMI in the FDG study in **a** brain, **b** liver, **c** blood and **d** muscle. The solid line interprets the linear fit of the data and dotted line represents 95% confidence interval of the model.

Fig. 5 Linear regression of different types of SUV measurements as a function of BMI in the PSMA study in **a** liver, **b** parotid gland, **c** blood, **d** muscle and **e** prostate. The solid line interprets the linear fit of the data and dotted line represents 95% confidence interval of the model.

Table 1. Characteristics of Recruited Patients

Table 2. LBM fraction calculated using Dixon, James and Janma models compared with DXA as reference standard

Table 3. Fitting results and dependent analysis of SUV vs. BMI in FDG study

Table 4. Fitting results and dependent analysis of SUV vs BMI in PSMA study

References

1. Park SY, Zacharias C, Harrison CM, Fan RE, Kunder CA, Hatami N, et al. Gallium 68 PSMA-11 PET/MR Imaging in Patients with Intermediate- or High-Risk Prostate Cancer. Radiology. 2018;288:495-505. doi:10.1148/radiol.2018172232.
2. Hope TA, Fayad ZA, Fowler KJ, Holley D, Catana C. State of the Art PET/MRI: Applications and Limitations - Summary of the First ISMRM/SNMMI Co-Provided Workshop on PET/MRI. J Nucl Med. 2019;60:jnumed.119.227231. doi:10.2967/jnumed.119.227231.
3. Hoekstra CJ, Paglianiti I, Hoekstra OS, Smit EF, Postmus PE, Teule GJJ, et al. Monitoring response to therapy in cancer using [18F]-2-fluoro-2-deoxy-d-glucose and positron emission tomography: an overview of different analytical methods. Eur J Nucl Med. 2000;27:731-43. doi:10.1007/s002590050570.
4. Strauss LG, Conti PS. The Applications of PET in Clinical Oncology. The Journal of Nuclear Medicine. 1991;32:623-48. doi:10.1097/00004424-199104000-00018.
5. Zasadny KR, Wahl RL. Standardized uptake values of normal tissues at PET with 2-[fluorine-18]-fluoro-2-deoxy-D-glucose: variations with body weight and a method for correction. Radiology. 1993;189:847-50. doi:10.1148/radiology.189.3.8234714.
6. Kim CK, Gupta NC, Chandramouli B, Alavi A. Standardized Uptake Values of FDG: Body Surface Area Correction is Preferable to Body Weight Correction. Journal of Nuclear Medicine Official Publication Society of Nuclear Medicine. 1994;35:164-7.
7. Sugawara Y, Zasadny KR, Neuhoff AW, Wahl RL. Reevaluation of the Standardized Uptake Value for FDG: Variations with Body Weight and Methods for Correction1. Radiol. 1999. doi:10.1148/radiology.213.2.r99nv37521.
8. Menda Y, Bushnell DL, Madsen MT, Mclaughlin K, Kahn D, Kernstine KH. Evaluation of various corrections to the standardized uptake value for diagnosis of pulmonary malignancy. Nucl Med Commun. 2001;22:1077. doi:10.1097/00006231-200110000-00004.
9. Lowe VJ, Fletcher JW, Gobar L, Lawson M, Kirchner P, Valk PE, et al. Prospective investigation of positron emission tomography in lung nodules. Journal of Clinical Oncology Official Journal of the American Society of Clinical Oncology. 1998;16:1075. doi:10.1016/j.polymer.2011.04.018.
10. James WPT. Research on obesity. Nutr Bull. 1977. doi:10.1111/j.1467-3010.1977.tb00966.x.
11. Tahari A, Chien D, Azadi J, Wahl RL. Optimum Lean Body Formulation for Correction of Standardized Uptake Value in PET Imaging. The Journal of Nuclear Medicine. 2014;55:1481-4. doi:10.2967/jnumed.113.136986.
12. Janmahasatian S, Duffull DSB, Ash S, Ward LC, Byrne NM, Green B. Quantification of Lean Bodyweight. Clin Pharmacokinet. 2005;44:1051-65. doi:10.2165/00003088-200544100-00004.
13. Hu HH, Chen J, Shen W. Segmentation and quantification of adipose tissue by magnetic resonance imaging. Magnetic Resonance Materials in Physics Biology & Medicine. 2016;29:259-76. doi:10.1007/s10334-015-0498-z.
14. Ulbrich EJ, Nanz D, Leinhard OD, Marcon M, Fischer MA. Whole-body adipose tissue and lean muscle volumes and their distribution across gender and age: MR-derived normative values in a normal-weight Swiss population. Magn Reson Med. 2017. doi:10.1002/mrm.26676.
15. Karlsson A, Rosander J, Romu T, Tallberg J, Leinhard OD. Automatic and quantitative

assessment of regional muscle volume by multi ` tlas segmentation using whole‐body water–fat MRI. J Magn Reson Imaging. 2015;41. doi:10.1002/jmri.24726.
16. Kim WH, Kim CG, Kim D-W. Comparison of SUVs Normalized by Lean Body Mass Determined by CT with Those Normalized by Lean Body Mass Estimated by Predictive Equations in Normal Tissues. Nucl Med Mol Imaging (2010). 2012;46:182-8. doi:10.1007/s13139-012-0146-8.
17. Dixon, T W. Simple proton spectroscopic imaging. Radiology. 1984;153:189-94. doi:10.1148/radiology.153.1.6089263.
18. Jochimsen T, Schulz J, Busse H. Lean body mass correction of standardized uptake value in simultaneous whole-body positron emission tomography and magnetic resonance imaging. Phys Med Biol. 2015;60:4651-64. doi:10.1088/0031-9155/60/12/4651.
19. Vriens D, De Geus-Oei LF, Van Laarhoven HW, Timmer-Bonte JNH, Krabbe PFM, Visser EP, et al. Evaluation of different normalization procedures for the calculation of the standardized uptake value in therapy response monitoring studies. Nucl Med Commun. 2009;30:550. doi:10.1097/MNM.0b013e32832bdc80.
20. Erselcan T, Turgut B, Dogan D, Ozdemir S. Lean body mass-based standardized uptake value, derived from a predictive equation, might be misleading in PET studies. Eur J Nucl Med Mol Imaging. 2003;29:1630-8. doi:10.1007/s00259-002-0974-3.
21. Mazess RB, Barden HS, Bisek JP, Hanson J. Dual-energy X-ray absorptiometry for total-body and regional bone-mineral and soft-tissue composition. Am J Clin Nutr. 1990:1106-12. doi:10.1093/ajcn/51.6.1106.
22. Webber CE. Reproducibility of DXA Measurements of Bone Mineral and Body Composition: Application to Routine Clinical Measurements: Springer New York; 2012.
23. Prior BM, Cureton KJ, Modlesky CM, Evans EM, Sloniger MA, Saunders M, et al. In vivo validation of whole body composition estimates from dual-energy X-ray absorptiometry. J Appl Physiol. 1997;83:623. doi:10.1152/jappl.1997.83.2.623.
24. Rausch, Ivo, Rust, Petra, Beyer, Thomas, et al. Reproducibility of MRI Dixon-Based Attenuation Correction in Combined PET/MR with Applications for Lean Body Mass Estimation. J Nucl Med. 2016.
25. Borga M, West J, Bell J, Harvey N, Romu T, Heymsfield S. Advanced body composition assessment: from body mass index to body composition profiling. J Investig Med. 2018. doi:10.1136/jim-2018-000722.
26. Neeland IJ, Grundy SM, Li X, Adams-Huet B, Vega GL. Comparison of visceral fat mass measurement by dual-X-ray absorptiometry and magnetic resonance imaging in a multiethnic cohort: the Dallas Heart Study. Nutr Diabetes. 2016;6:e221. doi:10.1038/nutd.2016.28.
27. Liu G, Cao T, Hu L, Zheng J, Pang L, Hu P, et al. Validation of MR-Based Attenuation Correction of a Newly Released Whole-Body Simultaneous PET/MR System. BioMed Research International. 2019;2019:1-10. doi:10.1155/2019/8213215.
28. Gafita A, Calais J, Franz C, Rauscher I, Wang H, Roberstson A, et al. Evaluation of SUV normalized by lean body mass (SUL) in 68Ga-PSMA11 PET/CT: a bi-centric analysis. EJNMMI Research. 2019;9:103. doi:10.1186/s13550-019-0572-z.
29. Virtanen KA, Lidell ME, Orava J, Heglind M, Westergren R, Niemi T, et al. Functional Brown Adipose Tissue in Healthy Adults. N Engl J Med. 2009;360:1518-25. doi:10.1056/NEJMoa0808949.
30. Yeung HWD, Grewal RK, Gonen M, Schöder H, Larson SM. Patterns of (18)F-FDG uptake in adipose tissue and muscle: a potential source of false-positives for PET. J Nucl Med. 2003;44:1789-96.

Figures

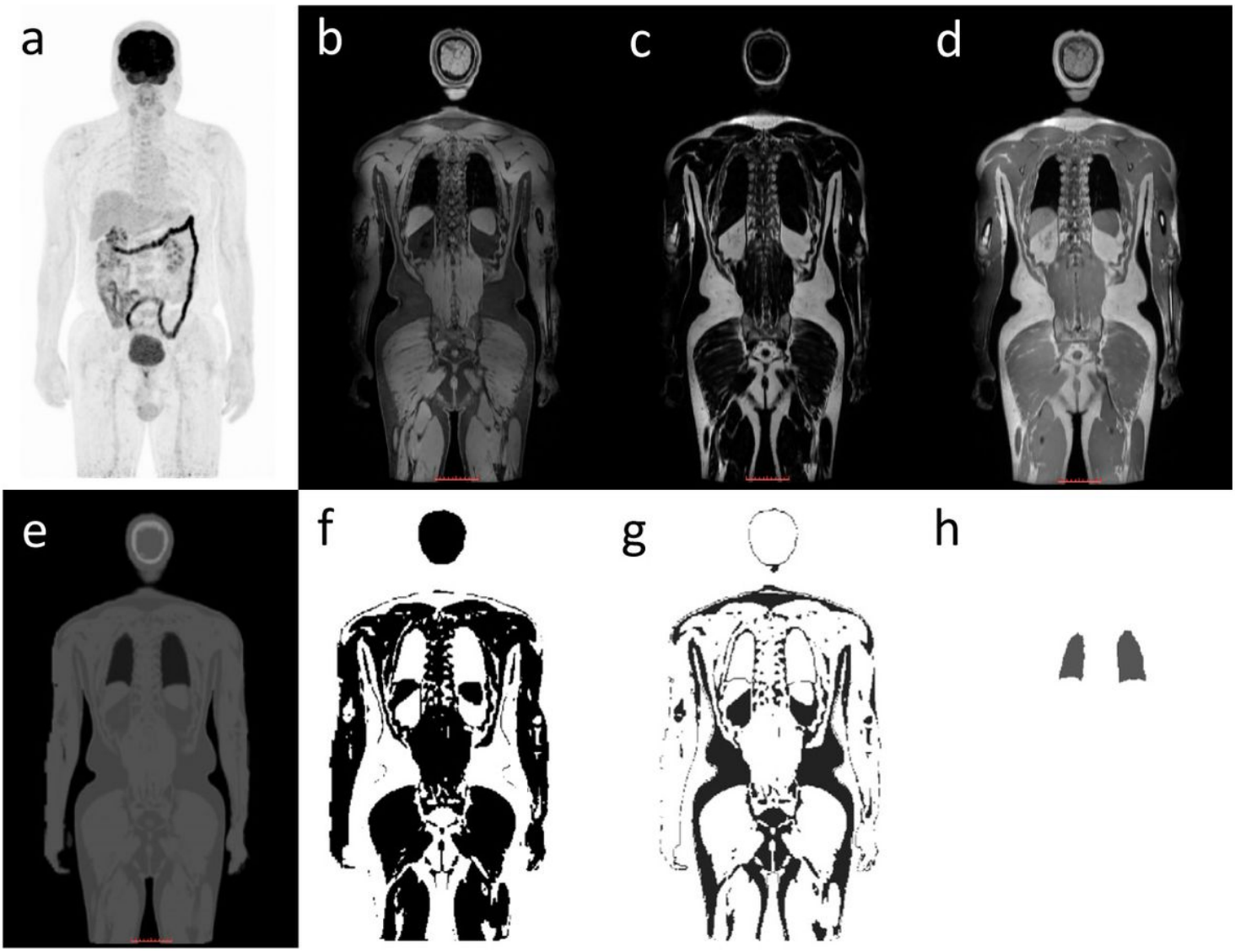

Figure 1

Representative images from a 18F-FDG PET/MR scan. a PET MIP, b water image, c fat image, d in-phase image, e MRAC map, f water segmented from MRAC, g fat segmented from MRAC and h lung segmented from MRAC.

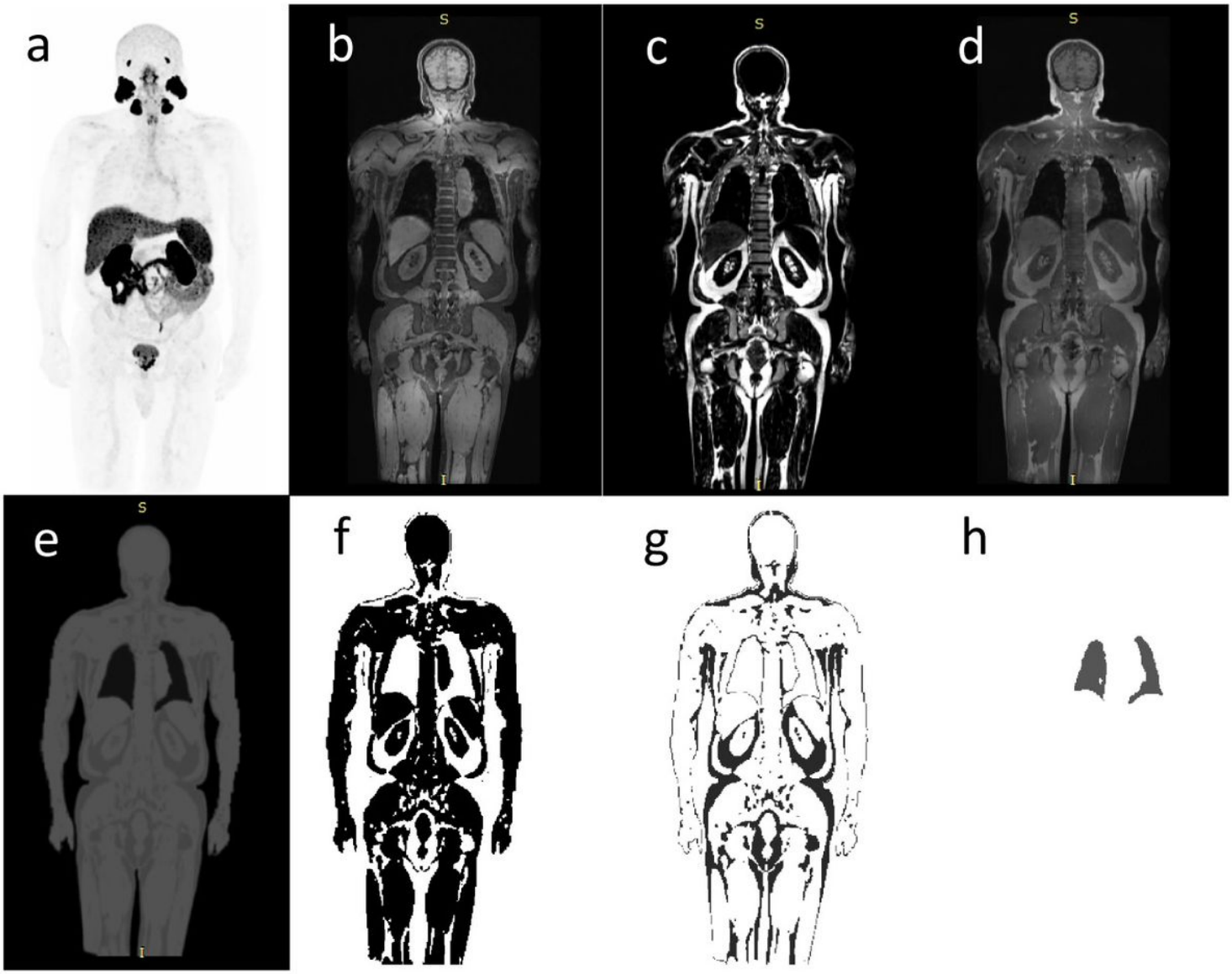

Figure 2

Representative images from a 18F-PSMA PET/MR scan. a PET MIP, b water image, c fat image, d in-phase image, e MRAC map, f water segmented from MRAC, g fat segmented from MRAC and h lung segmented from MRAC.

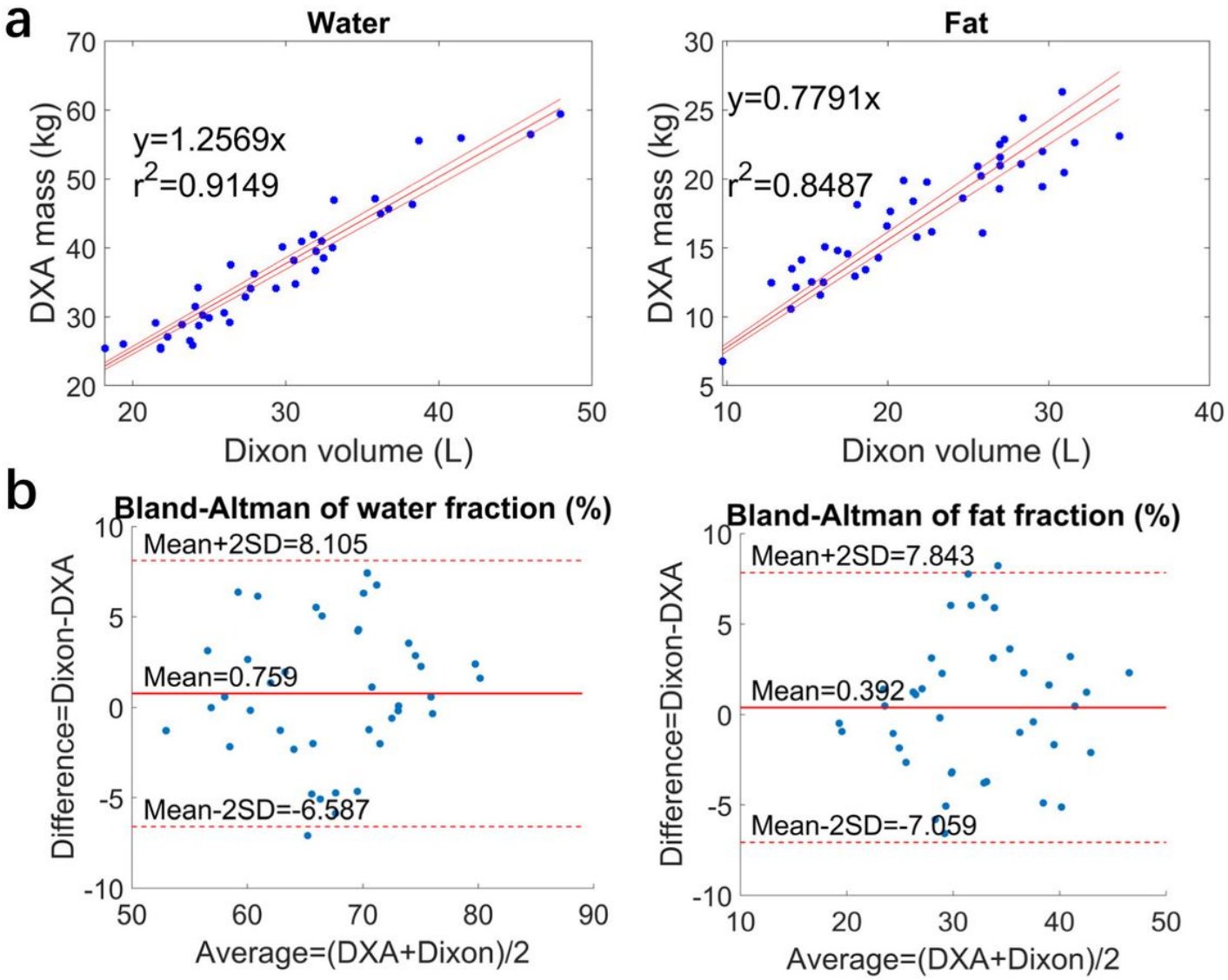

Figure 3

a: Linear regression of volume measured by Dixon vs. mass measured by DXA covering from head to upper thigh. The solid line interprets the linear fit of the data and dotted line represents 95% confidence interval of the model. b: Bland-Altman plot showing agreement between fat mass/bodyweight of DXA and Dixon measurements, and water mass/bodyweight of DXA and Dixon measurements.

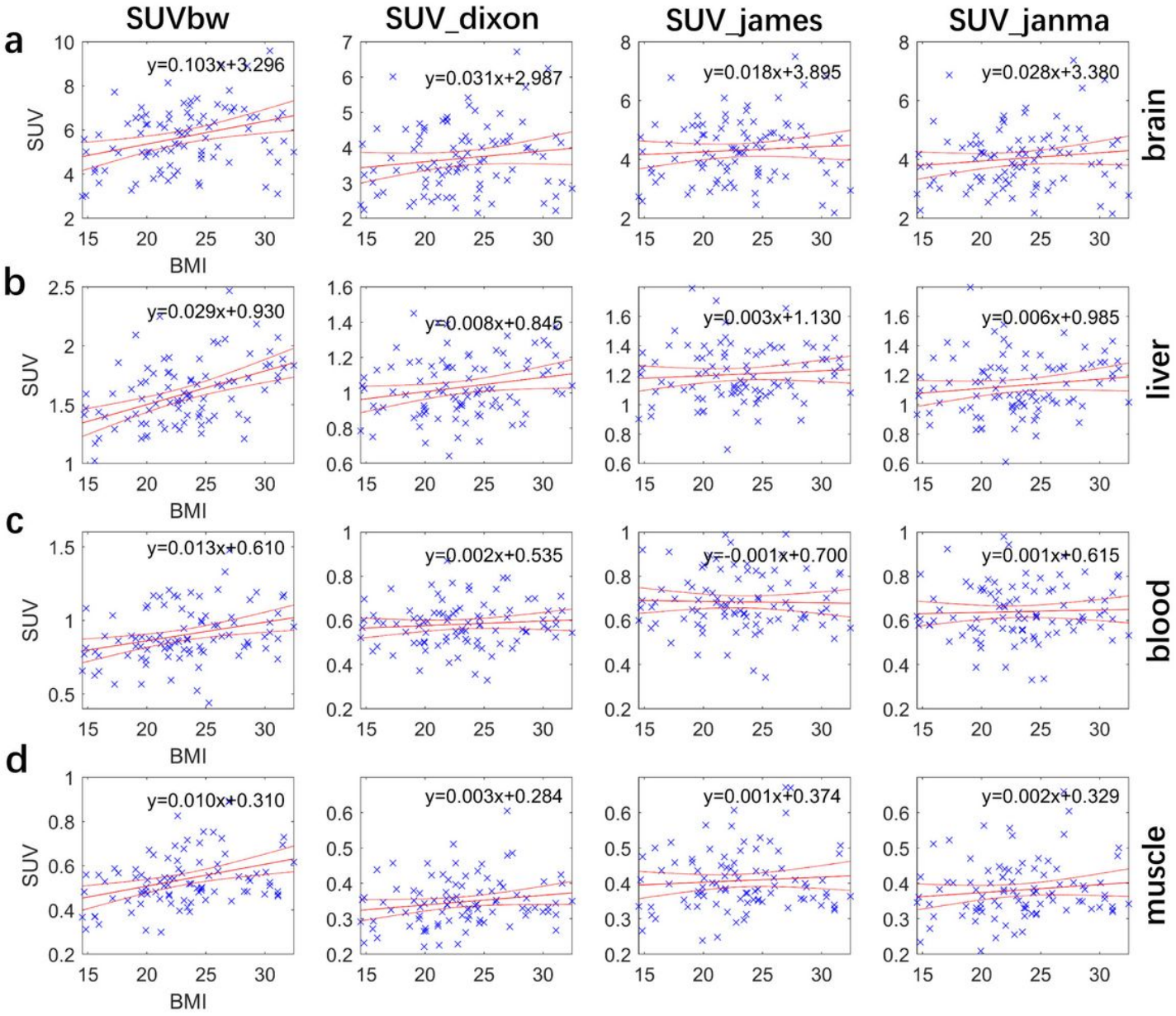

Figure 4

Linear regression of different types of SUV measurements as a function of BMI in the FDG study in a brain, b liver, c blood and d muscle. The solid line interprets the linear fit of the data and dotted line represents 95% confidence interval of the model.

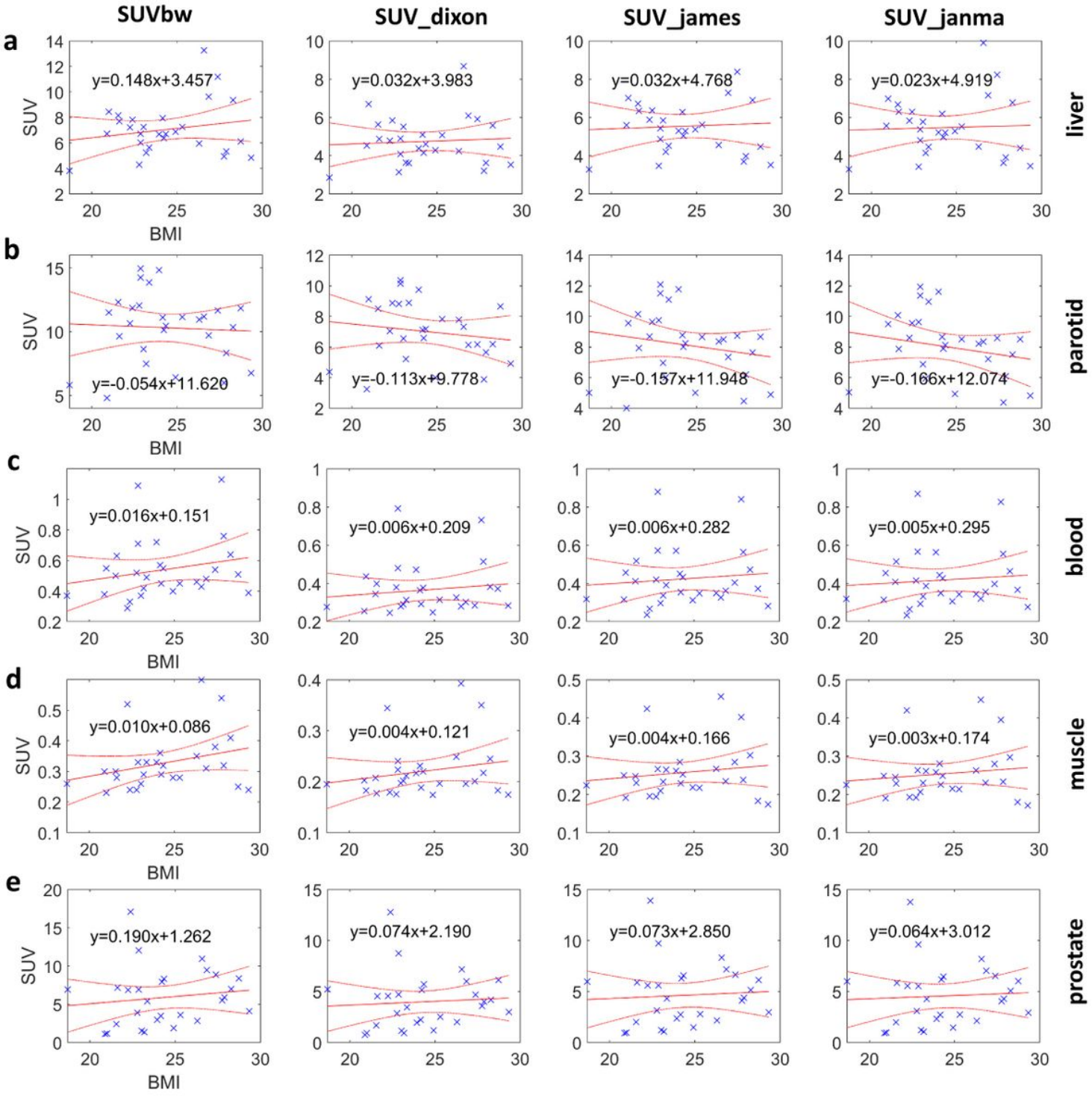

Figure 5

Linear regression of different types of SUV measurements as a function of BMI in the PSMA study in a liver, b parotid gland, c blood, d muscle and e prostate. The solid line interprets the linear fit of the data and dotted line represents 95% confidence interval of the model.